Regional Studies in Marine Science 102 (2026) 105360

Contents lists available at ScienceDirect

Regional Studies in Marine Science

journal homepage: www.elsevier.com/locate/rsma

First record of *Nitzschia traheaformis* in the Black Sea corrects the misidentification of toxigenic *N. navis-varingica* in the Sea of Marmara

Nickolai Davidovich [a,1,*], Olga Davidovich [a,2], Svetlana Polyakova [a,3], Elif Eker-Develi [b,4], Vyacheslav Yu. Nikulin [c,5], Arthur Yu. Nikulin [c,6]

[a] Karadag Scientific Station, Nature Reserve of the Russian Academy of Sciences, p/o Kurortnoe, Feodosiya 298188, Russia
[b] Mersin University, Faculty of Education, The Department of Mathematics and Science Education, Ciftlikkoy, Mersin 33343, Turkey
[c] Federal Scientific Center of the East Asia Terrestrial Biodiversity, Far Eastern Branch of the Russian Academy of Sciences, Vladivostok 690022, Russia

ARTICLE INFO

Keywords:
Cryptic speciation
Diatom biogeography
Integrative taxonomy
Nitzschia
Reproductive compatibility
Toxigenic species

ABSTRACT

Diatoms morphologically resembling the toxigenic species *Nitzschia navis-varingica* have been reported in the Sea of Marmara and the Mediterranean Sea, questioning its global spread. Using integrative taxonomy (biometrics, phylogenetics of *rbc*L, SSU and LSU rDNA, and mating experiments), we reassessed clones from populations from these basins and new isolates from the Black Sea. All clones belong to the *"Nitzschia traheaformis"* lineage. Our integrative approach not only provides the first confirmed record of *N. traheaformis* in the Black Sea—where it was likely overlooked due to its recent description and historical misidentification—but, more importantly, corrects the previous misidentification of *N. navis-varingica* in the Sea of Marmara, a finding with direct implications for regional biotoxin risk assessment and harmful algal bloom monitoring. Reproductive experiments revealed that Black Sea and Sea of Marmara populations are reproductively compatible, suggesting they belong to the same biological species. Mediterranean clones exhibited only rare homothallic reproduction, preventing a conclusive assessment of their relationship to other populations. Thus, our results demonstrate that the isolates examined from the Black Sea, the Sea of Marmara, and, based on our molecular data, the Mediterranean basin belong to the *N. traheaformis* lineage—for which no toxicity has been reported to date—rather than the hazardous *N. navis-varingica*. This study underscores the critical importance of integrative taxonomy in uncovering easily misidentified or taxonomically challenging diatom species that require high-level morphological expertise for reliable discrimination, with direct implications for the accurate assessment of biotoxin risks and biodiversity trends.

1. Introduction

Cryptic speciation is widespread in diatoms, with morphologically similar but genetically distinct lineages often occupying disparate geographic ranges (Kaczmarska et al., 2014; Amato et al., 2019). Cryptic and pseudo-cryptic species are now recognized in numerous diatom genera (Beszteri et al., 2005; Amato et al., 2007; Mann and Evans, 2008; Poulíčková et al., 2010; Lundholm et al., 2012; De Luca et al., 2021). Although closely related, these species can exhibit distinct physiological traits (Gallagher, 1982; Quijano-Scheggia et al., 2009). Such hidden diversity challenges traditional morphology-based identifications, particularly in *Nitzschia*, where high structural similarity of valve ornamentation and limited diagnostic characters complicate species delineation (Mann et al., 2021).

Nitzschia navis-varingica Lundholm et Moestrup, first described from a shrimp pond in Vietnam (Lundholm and Moestrup, 2000), is a diatom

* Corresponding author.
E-mail address: nickolaid@yandex.ru (N. Davidovich).
[1] https://orcid.org/0000-0002-3510-0453
[2] https://orcid.org/0000-0003-3768-5878
[3] https://orcid.org/0000-0002-1551-3031
[4] https://orcid.org/0000-0003-0174-1903
[5] https://orcid.org/0000-0002-6643-4325
[6] https://orcid.org/0000-0001-6113-2136

https://doi.org/10.1016/j.rsma.2026.105360
Received 6 February 2026; Received in revised form 10 August 2026; Accepted 13 August 2026
Available online 19 August 2026

of ecological and economic concern due to its production of domoic acid—a neurotoxin linked to amnesic shellfish poisoning in humans and mass mortality events in marine fauna (Kotaki et al., 2000; Lefebvre and Robertson, 2010). Originally reported across the Western Pacific (Kotaki et al., 2004; Romero et al., 2008; Suriyanti and Usup, 2015; Tan et al., 2016; Puilingi et al., 2022), its conjectural expansion into the Mediterranean Sea (Ayaz et al., 2018) and the Sea of Marmara (Eker-Develi and Kideys, 2022) raises a critical biogeographic question: Is this a true cosmopolitan invasion, or should distant populations be attributed to a species complex, wherein morphologically similar entities are subsumed under a single name?

The three basins investigated in this study—the Black Sea, the Sea of Marmara, and the northeastern Mediterranean Sea—are hydrologically connected but differ markedly in their physicochemical properties. The Black Sea is a permanently stratified basin with a surface salinity of approximately 18‰, while the Mediterranean Sea is a typical oligotrophic marine system with surface salinities of 37–39‰ (Poulos, 2020, 2023). The Sea of Marmara serves as a transitional corridor between these basins, connected to the Black Sea via the Bosphorus Strait and to the Aegean Sea via the Dardanelles. Its upper 20–25 m layer is occupied by low-salinity Black Sea-origin waters (~24‰), while deeper layers are filled by denser, more saline Mediterranean waters (~38‰) (Poulos, 2023; Saçu et al., 2025a, 2025b). These oceanographic contrasts are essential for interpreting the taxonomic and biogeographical findings presented below. In addition, the oligotrophic conditions of the Mediterranean Sea contrast sharply with the more productive Black Sea basin, further contributing to the environmental heterogeneity of the region (Poulos, 2020).

Given the broad reported distribution of *N. navis-varingica*, geographically distant populations assigned to this species may represent a complex of cryptic taxa or be a result of misidentification. To resolve this taxonomic uncertainty for populations reported from the Mediterranean Sea and adjacent basins, we applied an integrative taxonomic approach. This study addressed the following principal questions: (i) Do the isolates from the Black Sea, the Sea of Marmara, and the Mediterranean Sea belong to *N. navis-varingica* or to a different lineage? (ii) What is the genetic and morphological relationship among these populations? (iii) Are populations from different basins reproductively compatible, and what does this reveal about species boundaries? To address these questions, we combined phylogenetic analyses based on nuclear (LSU and SSU rDNA) and plastid (*rbc*L) gene sequences, detailed morphological comparisons with published data for related species, and reproductive compatibility experiments following the Biological Species Concept (BSC; Dobzhansky, 1937; Mayr, 1942). The approach uses DNA sequence-based identification and phylogenetic analyses as complementary tools for species delimitation. This integrated strategy allowed us to rectify the misidentification of *N. navis-varingica* in the Sea of Marmara and to report the first record of *Nitzschia traheaformis* Li Ch., Witkowski & Yu Sh. in the Black Sea. Furthermore, it revealed distinct reproductive strategies among populations, highlighting the complex nature of speciation within this group.

2. Materials and methods

2.1. Sample collection and regional oceanographic setting

Black Sea samples were collected from two locations near the Crimean peninsula: Karadag (44.9111°N, 35.2032°E) and Sevastopol (44.6182°N, 33.5244°E) (Fig. 1). At Karadag, plankton samples were taken from the end of a pier approximately 100 m offshore using a small Jeddi net (25 cm mouth diameter, 74 μm mesh size) hauled vertically from a depth of 3 m, in three replicates. The total volume of filtered water was 0.442 m^3. Sampling was conducted in March 2023. At Sevastopol, samples were collected by scraping the surface of rocky substratum at a depth of 1 m, approximately 4 m offshore, in July 2023. At both Black Sea sites, water salinity was 18‰ as measured by a portable refractometer RHS−10ATC (China). The Black Sea is a permanently stratified basin with a surface salinity of approximately 18‰, and our samples were collected from the upper layer (Poulos, 2020, 2023).

Fig. 1. Location of sampling sites (open circles) in the seas of the Mediterranean basin.

Sea of Marmara samples were collected from two locations. Clones 23.0726-OL, 23.0820-SG, 23.0726-OP, 23.0726-OT, 23.0821-SD, and 23.0824-SM were derived from seawater samples collected from the upper 0.5 m of the water column with a bucket at Darica, Gebze (40.7542°N, 29.3916°E) on 22 June 2021 (distance from shore 1 m, water temperature 20°C, salinity 23‰). This site is located at the entrance to İzmit Bay (Körfez), a large eastern extension of the Sea of Marmara that receives substantial input of low-salinity Black Sea waters via the Bosphorus Strait. Additionally, at Istanbul (40.9699°N, 28.7902°E), samples were obtained by scraping the surface of rocky substratum at a depth of 0.5 m, approximately 2 m offshore, on 18 July 2023 (water temperature 23°C, salinity 22‰). Clones 23.0802-OA and 23.0802-OE were established from these isolates.

The Sea of Marmara is a strongly stratified two-layer system, with a low-salinity upper layer (Black Sea origin, ~22–24‰) occupying the upper 20–25 m, and a denser, high-salinity lower layer (Mediterranean origin, ~38‰) below a pronounced halocline (Poulos, 2023; Saçu et al., 22025a,2025b). All Sea of Marmara samples in this study were collected from the Black Sea-influenced upper layer. The two-layer exchanges through the Bosporus and Dardanelles straits connect these basins: Black Sea surface water flows southward through the Bosporus into the Sea of Marmara, while Mediterranean-origin water enters the Marmara as a lower-layer current; similarly, the Marmara upper layer exits through the Dardanelles into the Aegean Sea as a low-salinity surface plume, progressively mixing with surrounding waters (Beşiktepe et al., 1994; Poulos, 2020, 2023).

Mediterranean Sea samples were obtained from near-surface waters at Erdemli (36.6011°N, 34.3122°E) on 25 February 2016 at 1–1.5 m depth (distance from shore 15 m, water temperature 17°C, salinity 38‰), and at Mersin (36.7760°N, 34.5861°E) on 18 March 2022 at 1.5–2 m depth (distance from shore 60 m, water temperature 18°C, salinity 38‰). The northeastern Mediterranean Sea is a typical oligotrophic marine system with surface salinities of 37–39‰, and our samples were collected within the surface mixed layer (Poulos, 2020).

For the Sea of Marmara (except clones 23.0802-OA and 23.0802-OE) and Mediterranean Sea samples, initial cultures were established from single-cell isolations by Elif Eker-Develi. Subsequently, to ensure

monoclonal status, re-isolation was performed at the Karadag laboratory by picking single cells from these initial cultures. In the laboratory, single cells were isolated using the micropipetting technique (Andersen and Kawachi, 2005) under an inverted optical microscope Nib−100 (Biobase, China).

A total of 21 clones were established: four from the Black Sea (23.0320-SC, 23.0715-SP, 23.0715-SK, 24.0315-OL), eight from the Sea of Marmara (23.0726-OL, 23.0820-SG, 23.0726-OP, 23.0726-OT, 23.0802-OA, 23.0802-OE, 23.0821-SD, 23.0824-SM), and nine from the Mediterranean Sea (23.0725-OE, 23.0801-OL, 23.0801-OK, 23.0801-OM, 23.0801-ON, 23.0725-OF, 23.0725-OJ, 23.0725-OG, 23.0918-SP). Later, two additional clones, 24.0408-OG1 and 24.0408-OL1, were obtained as descendants following intraclonal auxosporulation of clones 24.0408-OG and 24.0408-OL, respectively. Detailed clone provenance and metadata are provided in Table 2 and Supplementary Table S1.

2.2. Cultivation, observations, and mating experiments

Cultures used for mating experiments were maintained in the ESAW culture medium (Andersen et al., 2005) with modifications (Polyakova et al., 2018) under natural dim light from a north-facing window, avoiding direct sunlight, at a temperature of approximately 20°C. The levels of salinity used for growing cultures were chosen to approximate the source environments of each regional group (18‰ for the Black Sea, 24‰ for the Sea of Marmara to represent its typical upper-layer salinity, and 38‰ for the Mediterranean Sea).

Mating experiments were performed with exponentially growing clones under the same culture conditions except for salinity levels. Native salinities were used for intrapopulation mating. Intermediate salinity levels (21‰ for Black Sea–Sea of Marmara crosses, 28‰ for Black Sea–Mediterranean crosses, and 31‰ for Sea of Marmara–Mediterranean crosses) were used for interpopulation mating. In the latter case, clones were acclimated to intermediate salinity over one week. Clones were pairwise mixed in Petri dishes 5 cm in diameter and monitored daily for 5 days for the appearance of gametes, zygotes, and auxospores. The first confirmed reproductively compatible pairs of clones served as a control for subsequent crosses with the remaining clones. In case of a negative result, the crossing was repeated 3–4 times. The clones used in experiments were in the generative phase of their life cycle, as indicated by their cell size being half or less of the species-specific maximum (Davidovich, 2001).

Living cells were observed at 600 × magnification using a BiOptic CI−300 (Bioptic LLC, Russia) light microscope (LM) equipped with differential interference contrast (DIC) optics. LM photographs were taken with an E3ISPM08300KPC C-mount USB3.0 CMOS camera (ToupTek Photonics, China). For scanning electron microscopy (SEM), a cell suspension was boiled in hydrogen peroxide for four hours and then rinsed 7–8 times with distilled water. A drop of the cleaned cell suspension was placed on aluminium stubs and allowed to dry at room temperature. Stubs were sputter-coated with gold. SEM was performed using a Hitachi SU8020 (Japan) microscope. Cell dimensions were measured for each population (the Black Sea, the Sea of Marmara, and the Mediterranean Sea). Apical size (length) was determined for a minimum of 200 cells, and transapical size (width) for a minimum of 50 cells per population. For the Black Sea and the Sea of Marmara populations, stria density (per 10 μm) was calculated using 20 cells, and fibulae density using 10 cells.

2.3. DNA analysis

For DNA analysis, the unialgal cultures were harvested during the exponential growth phase and concentrated by centrifugation. Total genomic DNA was extracted according to Abdullin et al. (2021). PCR amplification of the plastid-encoded *rbc*L gene region, nuclear-encoded small subunit ribosomal RNA gene (SSU rDNA), and large subunit ribosomal RNA gene (LSU rDNA) was carried out using primers: DPrbcL1 and DPrbcL7 (Daugbjerg and Andersen, 1997); 18SP2F and 18SP4R (van Hannen et al., 1999; Guillou et al., 1999); and D1R and T24U (Scholin et al., 1994; Harper and Saunders, 2001), respectively, with the Encyclo Plus PCR kit (Evrogen, Russia). Amplification reactions for SSU and LSU rDNA followed this thermal profile: 95°C for 2 min, followed by 40 cycles of denaturation at 95°C for 15 s, annealing at 55°C for 15 s, and extension at 72°C for 90 s. After the cycles, the final extension was completed at 72°C for 7 min. For the *rbc*L gene, the thermal profile was: 95°C for 2 min, 40 cycles (95°C for 15 s, 46°C for 15 s, 72°C for 90 s), and 72°C for 7 min. The PCR products were purified with ExoSAP-IT PCR Product Cleanup Reagent (Affymetrix, USA) and sequenced in both directions using an ABI 3500 genetic analyzer (Applied Biosystems, USA) at the Instrumental Center of Biotechnology and Gene Engineering of FSCEATB FEB RAS with a BigDye Terminator v3.1 sequencing kit (Life Technologies Corporation, USA) and the same primers used for PCR. Sequences were assembled using the Staden Package v. 1.4 (Bonfield et al., 1995). The sequences (taxa and accession numbers are given in the tree) were aligned in the SeaView program (Galtier et al., 1996).

Five datasets were used to clarify the phylogenetic position of the studied clones: (1) an SSU rDNA alignment based on the dataset of Mann et al. (2021), including 116 sequences (1665 bp), with *Eunotia* Ehrenberg sequences used as the outgroup; (2) an *rbc*L cpDNA alignment based on the dataset of Mann et al. (2021), including 98 sequences (1385 bp), with *Eunotia* sequences used as the outgroup; (3) a reduced *rbc*L dataset (21 sequences; 1385 bp) representing the "*N. traheaformis*" lineage, with *N. linearis* W. Smith (strain Nit53) and *N. dubiiformis* Hustedt (strain s0311) used as the outgroup; (4) an LSU rDNA alignment (94 sequences; 762 bp) based on the dataset of Tan et al. (2025), with *Eunotia* sequences used as the outgroup; (5) a reduced LSU rDNA dataset (83 sequences; 740 bp), representing the "*N. traheaformis*" and "*Nitzschia navis-varingica*" lineages. The datasets were enriched with all accessions that showed the highest sequence similarity to the sequences obtained from our strains, as inferred from BLAST searches (https://blast.ncbi.nlm.nih.gov/Blast.cgi). For our clones, *rbc*L, SSU rDNA, and LSU rDNA sequences have been deposited in GenBank under accession numbers PV536175–PV536184, PV523254–PV523260, and PX457424–PX457429 respectively. The full list is provided in Supplementary Table S1.

To determine the most appropriate DNA substitution models for the datasets, the Akaike information criterion (AIC; Akaike, 1974) was implemented in jModelTest 2.1.1 (Darriba et al., 2012). Phylogenetic trees were reconstructed using maximum likelihood (ML) in RAxML-NG (Kozlov et al., 2019) and Bayesian inference (BI) in MrBayes v.3.1.2 (Ronquist and Huelsenbeck, 2003). For the BI analysis, four parallel MCMC runs were performed for four million generations (SSU rDNA, *rbc*L), two million generations (LSU rDNA), and one million generations (reduced LSU rDNA and *rbc*L datasets), with sampling every 100 generations. Chain convergence and stationarity were assessed using the 'sump' plot, with the first 25% of samples discarded as burn-in. Posterior probabilities were calculated from the remaining trees sampled during the stationary phase. The convergence of the stationary distribution was assessed using ESS values (> 200) in Tracer v.1.7.1 (Rambaut et al., 2018). The robustness of the ML trees was evaluated by bootstrap percentages (BP) using the rapid bootstrap algorithm (Stamatakis et al., 2008) with 1000 bootstrap replicates. To evaluate relationships among LSU rDNA ribotypes, a TCS network was constructed in PopART v.1.7 (Leigh and Bryant, 2015) with the parameter Epsilon (ε) set to 0. Pairwise distances (*p*-distances) were calculated using MEGA 11 (Tamura et al., 2021).

Taxonomic nomenclature and authorities of all taxa mentioned in the manuscript were verified against the World Register of Marine Species (WoRMS; https://www.marinespecies.org) and AlgaeBase (https://www.algaebase.org).

3. Results

3.1. Morphological analyses and biometry (Table 1)

Nitzschia traheaformis from the Black Sea (Figs. 2, 3, 4).

Nitzschia traheaformis was identified in the Black Sea for the first time. The cells are solitary, each containing two chloroplasts positioned at opposite ends of the cell. In valve view, cells are lanceolate, while in girdle view they are rectangular, with the slightly indented central part. The apical size (length) ranged from 18 μm in the smallest cells observed to 92 μm in the initial cells resulting from sexual reproduction. The transapical size (width) ranged from 5 to 9 μm. The raphe is eccentric, raised on a keel and possesses a central nodule. The distance between fibulae is variable, with the greatest distance occurring between the two median fibulae. There are 32–39 striae and 11–17 fibulae in 10 μm.

Nitzschia traheaformis from the Sea of Marmara (Fig. 5, Figs S1–S4) = *Nitzschia navis-varingica* sensu Eker-Develi and Kideys (2022)

Morphologically, individuals from the Sea of Marmara are similar to the ones isolated from the Black Sea in terms of cell shape, length (21–79 μm; the maximum length refers to the initial cells resulting from mating between the Sea of Marmara and Black Sea populations), width (4–13 μm), number of striae (30–39 in 10 μm) and fibulae (9–18 in 10 μm). The areolae are circular, with a density of approximately 5–6 in 1 μm. Externally, interstriae are raised, while internally they are smooth. The number of striae between two fibulae in the central area was about 6–8, whereas in other areas, it varied between 1 and 3. A single row of areolae is present in the raphe canal.

***Nitzschia navis-varingica* sensu Ayaz et al. (2018) from the Mediterranean Sea** (Fig. 6, Figs S5–S11)

The average cell lengths of the Mediterranean Sea isolates (26 ± 2.5, n = 217 and 27 ± 4.7, n = 254, obtained from samples taken on 25 February 2016 and 18 March 2022, respectively) were shorter than that of the Sea of Marmara isolate (40 ± 8.5, n = 272, obtained from the 22 June 2021 sampling). Overall cell shape was similar in all three regions. The number of striae and fibulae was 34–36 and 14–15 per 10 μm, respectively. Cells are larger in girdle view than in valve view. The maximal cell length after intraclonal auxosporulation was 66 μm. The number of striae between the two fibulae in the central interspace was 4–7. Sometimes, the central interspace was not present. Excluding the central interspace, the number of striae between fibulae varied between 1 and 3. A terminal fissure is seen at the distal end of the raphe in the external view. The number of areolae in 1 μm is ~5–6. A single row of areolae is present in the raphe canal. The structure of the girdle bands is similar in the Mediterranean and the Sea of Marmara isolates. There are silica warts on the girdle bands and on the mantle. There are also silica ridges on the mantle. However, silica ridges are not apparent on the raphe canal. One or two rows of striae are present on each girdle band.

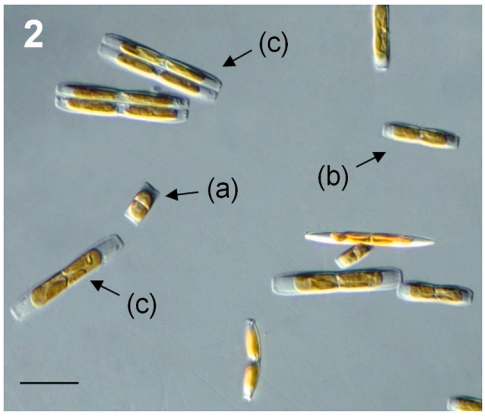

Fig. 2. *Nitzschia traheaformis* from the Black Sea. Live cells of two sexually compatible parental clones, 23.0320-SC (a) and 23.0715-SK (b), differing in cell size, and progeny (post-initial) cells (c) resulting from heterothallic sexual reproduction. Light microscopy (LM), differential interference contrast (DIC). Scale bar: 20 μm.

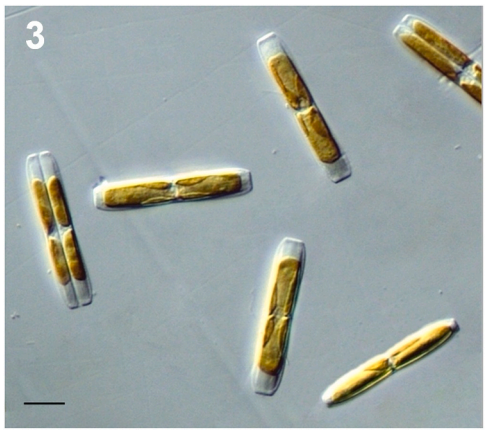

Fig. 3. Dividing cells disperse after completion of division without forming any ribbon-like colonies. LM, DIC. Scale bar: 20 μm.

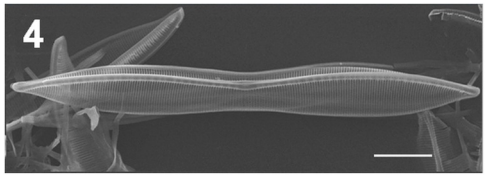

Fig. 4. *Nitzschia traheaformis* (clone 23.0320-SC) from the Black Sea. SEM. Scale bar: 5 μm.

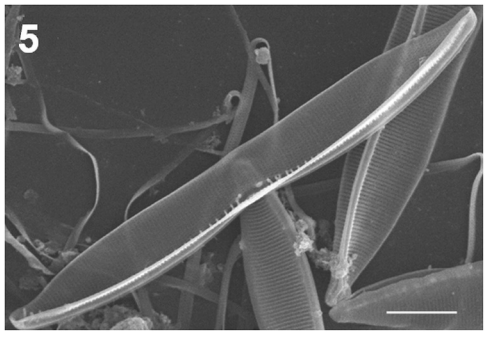

Fig. 5. *Nitzschia traheaformis* (clone 23.0824-SM) from the Sea of Marmara. SEM. Scale bar: 5 μm.

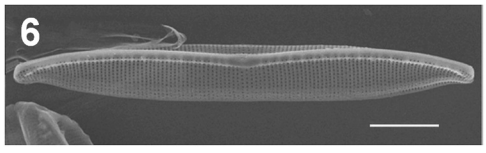

Fig. 6. Clone 23.0918-SP from the Mediterranean Sea, morphologically similar to *Nitzschia traheaformis*. SEM. Scale bar: 5 μm.

3.2. Sexual reproduction

Both homo- and heterothallic reproduction were observed in clones from the Black Sea and the Sea of Marmara, with heterothallic reproduction being strictly controlled by their mating types (Table 2). These populations exhibited both intra- and interpopulation mating.

Table 1
Biometry of diatoms morphologically similar to *Nitzschia navis-varingica* and *N. traheaformis* from different localities.

Population locality	Cell length, µm	Cell width, µm	Stria density, per 10 µm	Fibula density, per 10 µm	Peculiarity	Reference
Nitzschia navis-varingica group						
Vietnam (species type locality)	45–55	9–11	26–30	10–12	cells are generally single but occasionally occur as doublets or triplets	Lundholm and Moestrup, (2000)
Japan	38–110	9–11	26–29	10–12	most cells made ribbon-shaped colonies	Kotaki et al. (2004)
Philippines	38–110	9–11	26–30[a])	10–15	most cells made ribbon-shaped colonies	Kotaki et al. (2006)
Thailand	38–110	9–11	nd	nd	most cells make ribbon-shaped colonies	Romero et al. (2008)
Malaysia	43.5–75.7	3.6–6.7	25–27	7–9	cells form ribbon-like colonies	Suriyanti and Usup, (2015), Tan et al. (2016)
Mediterranean Sea (northeastern part)	40–50	7–14	~ 34	nd	cells are solitary	Ayaz et al. (2018)
Mediterranean Sea (northeastern part)	34–47	4–6	36	15	cells are solitary	Eker-Develi et al. (2020)
Papua New Guinea	38–110	9–11	nd	nd	most cells made ribbon-shaped colonies	Puilingi et al. (2022)
Western Pacific	55–216	5–18	nd	nd	nd	Tan et al. 2025[a]
Nitzschia traheaformis group						
Bohai Sea (species type locality)	17–54	3–4.7	32–34	11–14	nd	Witkowski et al. (2016)
Sea of Marmara	21–56	4–13	nd	nd	cells are solitary and occasionally as doublets	Eker-Develi and Kideys, (2022)
Tyrrhenian Sea	22–48	3.8–6	31–32	15–17	nd	Pelusi et al. (2025)
Sea of Marmara	13–79[b])	3–8	30–39	9–18	cells are solitary	our data
Black Sea	18–89[b])	5–9	32–39	11–17	cells are solitary	our data

Notes: [a]) authors reported material as "corresponded to the description" or "showed high morphological similarity to the type material"; [b]) the maximum size refers to the largest initial cell; the maximal size of initial cells from the interpopulation mating (Black Sea x Sea of Marmara) was 92 µm; nd, no data

Interpopulation mating was confirmed using cells from different clones that had markedly different cell sizes. Pairwise mating experiments between sexually compatible clones resulted in intensive auxosporulation, independent of their geographical origin. Intraclonal reproduction was rare and sporadic, as not all clones possessed this ability.

In contrast, Mediterranean clones (n = 9) exhibited exclusively rare and sporadic intraclonal auxosporulation, with no observed interclonal mating despite repeated crossing attempts (3–4 replicates per pair, monitored daily for 5 days). Intraclonal reproduction was extremely infrequent: in a Petri dish with a clonal culture containing thousands of cells, usually no more than 5–7 auxospores could be found. Only three of the nine available clones were sexually active, even though their cell sizes (15–40% of the maximum recorded size) were within the reproductive phase of the life cycle. Attempts to initiate sexual reproduction between Mediterranean clones and those from the Black Sea or the Sea of Marmara were unsuccessful under the tested conditions.

3.3. Phylogenetic analyses

Summary statistics for the five datasets are presented in Table 3. The SSU and LSU rDNA gene sequences were identical across all investigated clones. BLAST search results indicated that the clones were most similar (>99% identity) to accessions of *N. traheaformis*, *N. dubiiformis*, *N. dubia* W.Smith, *N. linearis* W.Smith, *N. pellucida* Grunow, *N. bilobata* W.Smith, and *N. navis-varingica* based on SSU rDNA sequences, and to *N. traheaformis* and *Nitzschia* cf. *dubiiformis* accessions (approximately 98% identity) based on *rbc*L sequences, and to *N. traheaformis* based on LSU rDNA sequences (100% identity).

All newly obtained partial LSU rDNA sequences from the Black Sea, the Mediterranean Sea, and the Sea of Marmara formed a well-supported clade (100/1.00) with the type strain of *Nitzschia traheaformis* (SZCZCH971) (Fig. 7). This clade corresponded to the "*N. traheaformis*" lineage and was phylogenetically distinct (94/0.99) from the *N. navis-varingica* lineage, represented by its type strain (VSP974–1).

The haplotype network based on LSU rDNA sequences (Fig. 8) comprised 26 ribotypes (H1–H26; Table S2). Newly obtained sequences, along with the type of *N. traheaformis*, belonged to a single ribotype (H1) and were separated from other species by 6–28 mutational steps. The closely related ribotype of *Nitzschia* cf. *promare* differed from the *N. traheaformis* ribotype (H1) by a *p*-distance of 0.81%. The ribotypes of *N. navis-varingica* (H12–H26) formed a compact yet internally diverse group, characterized by low divergence (1–3 mutational steps; *p*-distances 0.26%), and were distinct from the *N. traheaformis* ribotype. This group was connected to H1 by a long branch, indicating a considerable number of substitutions (at least 13) between the two lineages, corresponding to a 2.07% sequence divergence. Other taxa, such as *N. linearis* (H4–H5), *N. amabilis* (H6), *N. dubiiformis* (H7), *N. pellucida* (H9–H10), and *N. laevis* (H11), formed distinct groups, confirming their clear genetic distinctiveness.

Phylogenetic analysis based on the SSU rDNA dataset placed our clones within the "*N. traheaformis*" lineage (24 sequences; Fig. S12) of clade 4B-II, following the classification of Mann et al. (2021). However, this lineage has low statistical support (85/-) and also included sequences of *Nitzschia* cf. *dubiiformis* and *Nitzschia* sp. Genetic divergence within this ribosomal DNA region was low. The type strain of *N. traheaformis* (SZCZCH971) was grouped within this lineage, while the six accessions designated earlier as *N. navis-varingica* were clustered not only as distant strongly supported lineage (K0969 and K0620), but also as a part of *N. traheaformis* lineage or *N. pellucida* / *N. linearis* lineage. The K0969 and K0620 clones were previously found as a part of the "*N. navis-varingica*" lineage based on the LSU rDNA data and were identical to the type.

The full *rbc*L dataset showed the highest number of variable (518) and parsimony-informative sites (426) among the three markers (Table 3). Phylogenetic analyses based on this dataset also placed our clones within the "*N. traheaformis*" lineage (89/1.00 for BP/PP; 19 sequences; Fig. S13). This lineage also included sequences of *Nitzschia* cf. *dubiiformis* and *Nitzschia* sp. Similar to the SSU rDNA analyses, the 4B-II clade lacked statistical support. Three of the four clones from the Black Sea (24.0315-OL, 23.0715-SK, and 23.0715-SP) were identical to the type material of *N. traheaformis* (SZCZCH971) in the reduced *rbc*L dataset analysis (Fig. S14), while the remaining clone (23.0320-SC) formed a common haplotype with the clone from SoM (23.0824-SM). Other clones from the Sea of Marmara and the Mediterranean Sea exhibited slight genetic divergence from this type strain. A haplotype network could not be constructed for the *rbc*L region due to substantial differences in sequence lengths among representatives of the "*N. traheaformis*" lineage.

Table 2
Mating compatibility of clones morphologically similar to *Nitzschia navis-varingica* from three local populations.

Population	Clone name	mating type	Black Sea, Karadag	Black Sea, Sevastopol	Black Sea, Sevastopol	Sea of Marmara	Sea of Marmara	Sea of Marmara	Sea of Marmara	Sea of Marmara	Sea of Marmara	Sea of Marmara	Sea of Marmara	Mediterranean Sea	Mediterranean Sea	Mediterranean Sea	Mediterranean Sea	Mediterranean Sea	Mediterranean Sea	Mediterranean Sea	Mediterranean Sea	Mediterranean Sea
			23.0320-SC	23.0715-SP	23.0715-SK	23.0726-OL	23.0820-SG	23.0726-OP	23.0726-OT	23.0802-OA	23.0802-OE	23.0821-SD	23.0824-SM	23.0725-OE	23.0801-OL	23.0801-OK	23.0801-OM	23.0801-ON	23.0725-OF	23.0725-OJ	23.0725-OG	23.0918-SP
			mt2	mt2	mt1	mt2	mt2	mt1	mt1	mt1	mt1	mt1	mt1									
Black Sea, Karadag	23.0320-SC	mt2																				
Black Sea, Sevastopol	23.0715-SP	mt2	0																			
Black Sea, Sevastopol	23.0715-SK	mt1	X	X																		
Sea of Marmara	23.0726-OL	mt2	0	0	X	I																
Sea of Marmara	23.0820-SG	mt2	0	0	X	0																
Sea of Marmara	23.0726-OP	mt1	X	X	0	X	X	I														
Sea of Marmara	23.0726-OT	mt1	X	X	0	X	X	0														
Sea of Marmara	23.0802-OA	mt1	X	n	n	n	n	n	n													
Sea of Marmara	23.0802-OE	mt1	X	n	n	n	n	n	n	n												
Sea of Marmara	23.0821-SD	mt1	X	X	0	X	X	0	0	n	n											
Sea of Marmara	23.0824-SM	mt1	X	X	0	X	X	0	0	n	n	0										
Mediterranean Sea	23.0725-OE		0	n	0	0	n	0	0	0	n	n	0	I								
Mediterranean Sea	23.0801-OL		0	n	0	0	n	0	0	0	n	n	0	0	I							
Mediterranean Sea	23.0801-OK		0	n	0	0	n	0	0	0	n	n	0	0	n							
Mediterranean Sea	23.0801-OM		0	n	0	0	n	0	0	0	n	n	0	0	0	0						
Mediterranean Sea	23.0801-ON		n	n	0	0	n	0	0	0	n	n	n	0	n	n	0					
Mediterranean Sea	23.0725-OF		0	n	0	0	n	0	0	0	n	n	0	0	n	0	0	n				
Mediterranean Sea	23.0725-OJ		0	n	0	0	n	0	0	0	n	n	0	0	0	n	0	n	0			
Mediterranean Sea	23.0725-OG		0	n	0	0	n	0	0	0	n	n	0	0	0	0	0	0	0	0	I	
Mediterranean Sea	23.0918-SP		n	0	0	0	0	n	0	0	n	0	0	0	n	0	n	n	0	0	0	

Notes: mt1 and mt2, mating types; X, interclonal reproduction; I, intraclonal reproduction; 0, no reproduction; n, no data; squares filled in yellow and red indicate intrapopulation and interpopulation mating, respectively

Table 3
Characteristics of the molecular markers used in this study.

Marker	Alignment length (bp)	Variable sites	Parsimony-informative sites	Substitution model	Number of sequences
*rbc*L	1385	518	426	GTR + I + G	98
*rbc*L (reduced dataset)	1385	142	70	TIM3 + I	21
SSU rDNA	1665	376	276	GTR + I + G	116
LSU rDNA	762	202	124	TIM3 + I + G	94
LSU rDNA (reduced dataset)	740	66	39	TrN + I + G	83

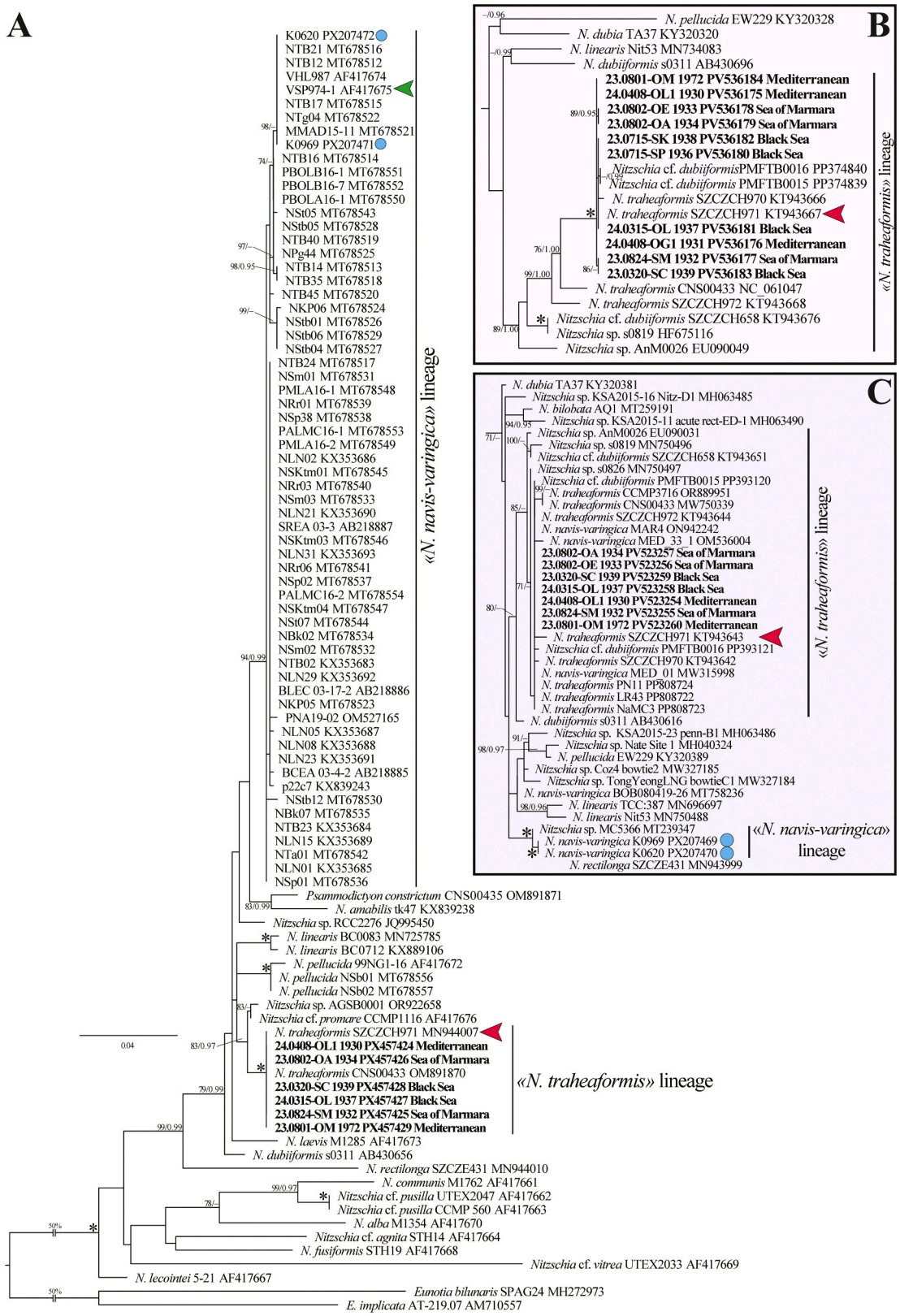

Fig. 7. Phylogenetic position of *Nitzschia* strains based on partial LSU rDNA sequences. (A) Maximum Likelihood (ML) tree (94 sequences; 762 bp alignment; best-fit model: TIM3+I+G). The outgroup branch is shortened by 50%. (B, C) The *N. traheaformis* clade from the supplementary (B) *rbc*L and (C) SSU rDNA trees (see Figs. S12, S14). Branch support values (ML bootstrap ≥ 70% / Bayesian posterior probability ≥ 0.95) are shown above branches. Asterisks indicate maximal support (100% bootstrap / 1.0 posterior probability). Newly sequenced strains are in bold. Symbols: red arrowhead for *N. traheaformis* type strain; green arrowhead for *N. navis-varingica* type strain; blue circles for the strains closely related to the *N. navis-varingica* type (K0620 and K0969).

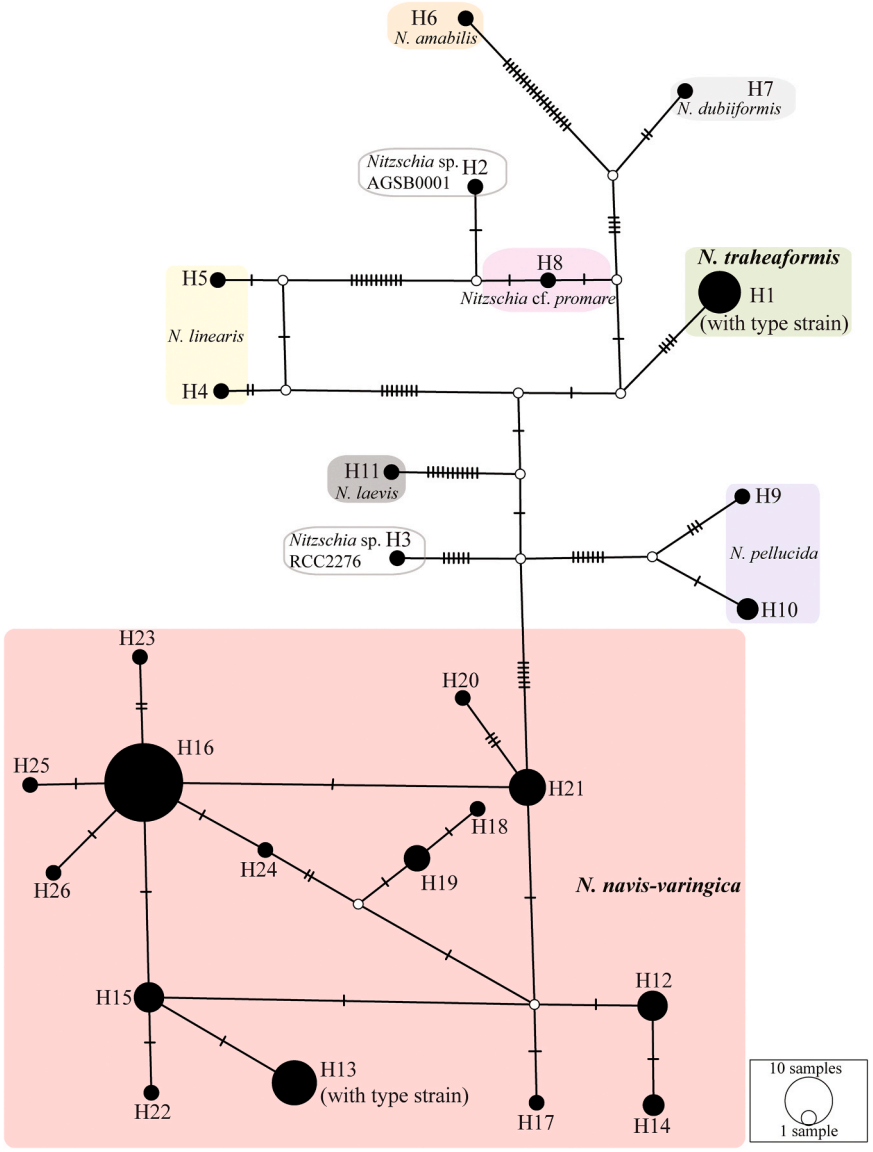

Fig. 8. Haplotype network of closely related *Nitzschia* species based on a 740-bp fragment of the LSU rDNA (83 sequences; 26 ribotypes). The network was constructed using the TCS network option. Small open circles represent hypothetical (unsampled) ribotypes. Circle size is proportional to the number of sequences assigned to each haplotype (see Supplementary Table S2). Hatch marks indicate the number of substitutions between nodes.

4. Discussion

4.1. Phylogenetic placement and species identification

Our data demonstrate that specimens from the Black Sea and the Sea of Marmara belong to *Nitzschia traheaformis,* a conclusion strongly supported by genetic analyses. Morphologically, the examined strains were broadly consistent with the description of the type material of *N. traheaformis* (Witkowski et al., 2016), although several ultrastructural characters varied or could not be resolved unambiguously. Nevertheless, our strains show only partial morphological similarity to other *Nitzschia* species, such as *N. dubiiformis*, *N. navis-varingica*, and *N. pellucida*. It should be noted that the SSU rDNA and *rbc*L phylogenies show a polyphyletic pattern for some named species in the complex (e.g., *N. dubiiformis*). This likely reflects a combination of historical misidentifications in public databases and the insufficient resolution of these markers to distinguish recently diverged lineages.

The three genetic markers used in this study provide complementary but different types of information, largely because of the differing availability of reference sequences for the two target species. SSU rDNA is highly conserved and exhibits little variation among closely related lineages, which explains the lack of statistical support for some clades (e.g., clade 4B-II). All our clones share identical sequences. This is consistent with the general observation that SSU rDNA has low resolution at the species level due to its conserved regions, which are often shared even among distantly related subdivisions (Moniz and Kaczmarska, 2009). In public databases, this marker contains sequences of both the *N. traheaformis* lineage and a lineage that, based on LSU rDNA data, corresponds to *N. navis-varingica* (K0969 and K0620). The inclusion of *N. navis-varingica* sequences from Turkey within the "*N. traheaformis*" clade—where they are nearly identical to our clones and the type strain—strongly suggests misidentification or incorrect annotation. Definitive confirmation would require voucher examination, but the genetic evidence consistently places them with *N. traheaformis*, not with the type strain of *N. navis-varingica*.

The plastid-encoded *rbc*L gene shows moderate variability; among our clones, four distinct haplotypes were detected. However, no *rbc*L sequences of verified *N. navis-varingica* (including its type strain) are available in GenBank, so this marker cannot be used to directly compare the two species. *rbc*L phylogeny suggests that two samples of *Nitzschia* cf.

dubiiformis (PMFTB0015 and PMFTB0016) from the Adriatic Sea belong to the *N. traheaformis* lineage. Therefore, we employed LSU rDNA, as it is currently the only marker for which reference sequences of both type strains—*N. traheaformis* (SZCZCH971) and *N. navis-varingica* (VSP974–1)—are publicly available. This allows unambiguous discrimination between the two lineages, with a clear genetic distance of 2.07%. All our clones share an identical LSU ribotype (H1) with the *N. traheaformis* type strain. All *N. navis-varingica* samples with available LSU rDNA sequences were collected from the Western Pacific Ocean (the Philippines, Malaysia, Vietnam, and Papua New Guinea), which is consistent with the species' type locality (Lundholm and Moestrup, 2000). LSU rDNA was the most informative marker for distinguishing the two lineages in the present dataset and under the current reference-sequence coverage**.** Taken together, these findings underscore the necessity of using multiple complementary markers, with due attention to the taxonomic coverage of reference sequences, alongside morphological and reproductive data to accurately delineate species boundaries in this complex.

A weak and statistically unsupported geographic grouping is observed only in the *rbc*L phylogeny, but this pattern may be an artefact of limited sampling or low marker resolution. Among our *N. traheaformis* isolates, LSU rDNA data show no geographic differentiation. The shared haplotype between the Black Sea and the Sea of Marmara samples is consistent with their geographical proximity, while the presence of a common haplotype between the Black Sea and the Yellow Sea is more notable.

4.2. Insights from reproductive compatibility and its limits

Furthermore, mating experiments revealed reproductive compatibility between the Black Sea population and a population from the Sea of Marmara, where the diatom was previously misidentified as *N. navis-varingica* (Eker-Develi and Kideys, 2022). Both intra- and interpopulation heterothallic sexual reproduction were vigorous when clones from these populations had compatible mating types and their cell length was within the sexually inducible size range. Notably, interpopulation mating yielded the largest cell observed in *N. traheaformis* (92 µm), slightly exceeding the size of the initial cells obtained from heterothallic intrapopulation reproduction. In accordance with the Biological Species Concept (Dobzhansky, 1937; Mayr, 1942) as applied to diatoms (Amato, 2010), this observed reproductive compatibility provides strong evidence that these two populations constitute a single biological species. In contrast, clones from the Mediterranean Sea population did not exhibit a heterothallic mode of sexual reproduction, making it impossible to assess their reproductive compatibility with the Black Sea and the Sea of Marmara populations.

The complete absence of heterothallic mating in Mediterranean clones, both among themselves and with clones from other basins, warrants consideration of alternative explanations, but it does not by itself demonstrate reproductive isolation. Several alternative explanations for the failure to observe heterothallic reproduction in Mediterranean clones must be considered. First, we may have sampled only one mating type, as heterothallic diatoms typically require complementary mating types for sexual reproduction. Second, the Mediterranean population may represent a cryptic species or an incipient lineage that has lost or modified its sexual reproduction system. Third, environmental or physiological factors—such as salinity adaptation or culture conditions—might have suppressed heterothallic reproduction, although all clones were maintained under standardized conditions and cell sizes were within the inducible range. While our data do not allow us to distinguish conclusively among these hypotheses, the absence of observed heterothallic mating highlights the potential for divergence within the *N. traheaformis* lineage and underscores the challenges of applying the Biological Species Concept to lineages with limited or absent heterothallic reproduction under laboratory conditions.

The environmental gradients across the studied basins may also inform the interpretation of these reproductive patterns. The reproductive compatibility between Black Sea (18‰) and Sea of Marmara (22–24‰) populations, coupled with their shared LSU ribotype, is consistent with the hydrological connection via the Bosphorus surface outflow and suggests that the salinity difference between these basins does not impose a strong reproductive barrier. By contrast, the marked environmental discontinuity between the Sea of Marmara (upper-layer salinity 22–24‰) and the northeastern Mediterranean Sea (surface salinity ~38‰), separated by the two-layer exchange through the Dardanelles and progressive mixing of the Marmara surface plume in the Aegean Sea, coincides with the absence of heterothallic reproduction observed in the Mediterranean clones (collected from Erdemli and Mersin). While our data do not establish causality, this correlation raises the hypothesis that the marked environmental discontinuity between the Sea of Marmara and the Mediterranean may act as a selective barrier, potentially driving the observed differences in reproductive strategy or incipient speciation. Testing this hypothesis will require laboratory experiments and population genomic analyses.

The oceanographic connectivity described above implies potential hydrological linkage between the Black Sea and the Sea of Marmara upper layers, but does not itself demonstrate contemporary gene flow, recent connectivity, or the direction of dispersal among the studied populations. However, the tychopelagic (benthoplanktonic) habit of *N. traheaformis*—recorded from both water-column and sediment samples (Witkowski et al., 2016) and consistent with its occurrence in plankton-net, bucket, and scraping samples in the present study—combined with this hydrological connectivity, makes passive dispersal by currents a plausible mechanism for gene flow among geographically distant populations.

The unavailability of Western Pacific clones precluded direct crossing experiments to confirm or refute conspecificity with Atlantic populations. Crossing experiments provide a direct and objective means to delineate species boundaries by testing reproductive compatibility. Nonetheless, the application of the BSC is constrained by its reliance on labour-intensive experiments and clonal cultures, as well as its inapplicability to asexual or homothallic lineages, such as the Mediterranean clones examined here. It is crucial to note that the genetic divergence observed in common phylogenetic markers (e.g., mitochondrial, ribosomal, or chloroplast genes), while useful for reconstructing evolutionary relationships, does not directly measure or predict reproductive isolation. These markers reflect the cumulative history of evolutionary change, which may or may not coincide with the emergence of pre- or post-zygotic barriers. Therefore, while our molecular data robustly place the Mediterranean clones within the *N. traheaformis* lineage, the absence of heterothallic mating under the tested conditions precludes any definitive conclusion about reproductive isolation and highlights the need for further investigation.

4.3. Morphological differentiation and phenotypic variability

To avoid future misidentifications of clones from Mediterranean and adjacent populations as *N. navis-varingica*, key morphological and biometric distinctions should be emphasised. In diatoms, the maximal cell size is typically restored during sexual reproduction (Chepurnov et al., 2004). The size of newly formed initial cells, though variable, approaches the maximum species-specific size. Therefore, *N. navis-varingica* from the Southeast Asia can be differentiated from the diatoms in the Black Sea and the Sea of Marmara based on their maximum cell dimensions (see Table 1). This distinction is further supported by differences in stria density between Western Pacific specimens and those from Mediterranean see and adjacent basins. In addition, unlike *N. navis-varingica* from the Southeast Asian populations, cells from the Black Sea and the Sea of Marmara did not form ribbon-shaped colonies during growth. The cells observed as doublets (e.g., Figs. 2 and 3) represent recently divided vegetative cells that have not yet separated.

The description of *N. traheaformis* by Witkowski et al. (2016) did not include a direct comparison with *N. navis-varingica*, and most studies employing an integrative approach have not analysed these two species simultaneously (Smida et al., 2014; Wang et al., 2022; Tan et al., 2025). However, a comparison of their size ranges clearly indicates dissimilarity (see Table 1). In addition, the following morphological characteristics help differentiate the two species: (1) the rows of poroids in the raphe canal are fewer in *N. traheaformis* (1–2 rows) than in *N. navis-varingica* (2–3 rows); (2) silica ridges on the wall of the raphe canal are present in *N. navis-varingica* but not apparent in *N. traheaformis*; (3) the central interspace is present and large in *N. traheaformis* (Witkowski et al., 2016), while it is either absent or replaced by half fibulae near the central nodule in *N. navis-varingica* (Lundholm and Moestrup, 2000; Tan et al., 2025); (4) vermiform silica ridges on the mantle are present in *N. navis-varingica* but have not been reported in *N. traheaformis*; and (5) silica warts on the girdle bands are reported for *N. navis-varingica* (Lundholm and Moestrup, 2000), whereas no information is available for *N. traheaformis* (Witkowski et al., 2016; Pelusi et al., 2025).

Based on the features 1 and 2, the isolates in the present study resemble *N. traheaformis*. However, other characteristics (items 3–5) do not fully align with its original description (Witkowski et al., 2016). Although a central interspace was observed in most of our specimens—consistent with *N. traheaformis*—the distance between the two central fibulae was narrower in the Black Sea, the Sea of Marmara and Mediterranean specimens (with 4–7 striae between them) as well as in those reported by Pelusi et al. (2025), than in the East Asian population (11 striae; Witkowski et al., 2016, Fig. 14). In our Mediterranean and Sea of Marmara specimens, silica warts on the mantle have been observed similar to the ones observed in *N. navis-varingica* (Lundholm and Moestrup, 2000). There were also vermiform silica ridges on the mantle in the Mediterranean isolates in the present study (Fig. S9) similar to the ones in *N. navis-varingica*. However, silica ridges on the wall of raphe canal were not apparent in any of the speciemens investigated in this study, as different from *N. navis-varingica*; however, we cannot exclude the possibility that these structures are present but were not resolved due to preparation or imaging limitations in *N. traheaformis* specimens in previous studies. These discrepancies may reflect phenotypic variation among geographically separated populations, highlighting the need for mating experiments between geographically distant strains of *N. traheaformis* to determine the extent of the species' phenotypic plasticity. Such experiments are crucial for taxonomic resolution, given that even reproductively compatible clones originating from a single population can exhibit considerable phenotypic and genetic divergence (Kaczmarska et al., 2009).

While our data confirm that the Black Sea and Sea of Marmara populations belong to the same biological species based on reproductive compatibility, the direction and mechanisms of dispersal among the studied basins remain unknown. The shared LSU rDNA ribotype (H1) across all studied populations—from the Black Sea and the Sea of Marmara to the Mediterranean Sea and the Yellow Sea (China)—might suggests recent common ancestry or ongoing gene flow, but this single marker lacks the resolution to distinguish between historical connectivity, recent introduction, or long-distance dispersal. The *rbc*L data further support this connection, with Black Sea clones sharing a haplotype with the type material from the Bohai Sea.

Several scenarios could explain the observed genetic connectivity across vast geographic distances. Ballast water transport is a plausible anthropogenic vector, given the heavy shipping traffic connecting the Black Sea, the Mediterranean, and East Asian ports. Alternatively, natural long-distance dispersal via marine currents cannot be excluded, particularly for a benthic diatom that may be resuspended into the water column. A third possibility is that *N. traheaformis* has a genuinely wide—possibly cosmopolitan—distribution that has been overlooked due to its recent description and morphological similarity to other species. The failure to observe heterothallic reproduction in Mediterranean clones under the tested conditions precludes a definitive assessment of their genetic exchange with northern populations.

Distinguishing among the dispersal hypotheses, clarifying the status of Mediterranean clones, and testing whether salinity gradients or other environmental factors drive local adaptation will require population genomic approaches and broader geographic sampling, particularly from the Western Pacific where both *N. navis-varingica* and *N. traheaformis* co-occur.

5. Conclusion

This study resolves the taxonomic identity of a diatom population previously misidentified as the toxigenic *Nitzschia navis-varingica* in the Sea of Marmara and confirms the presence of *N. traheaformis*—for which no toxicity has been reported to date—in the Black Sea, the Sea of Marmara, and, based on our molecular data, the northeastern Mediterranean Sea. Our integrative approach, combining morphology, phylogenetics, and mating experiments, was essential for this revision, as the high structural similarity among species in this complex renders morphology-based identification insufficient, and multi-gene analyses (particularly LSU rDNA) proved critical for species delimitation.

Reproductive experiments revealed that Black Sea and Sea of Marmara populations are reproductively compatible, consistent with their occurrence within hydrologically connected upper-layer waters via the Bosphorus surface outflow. In contrast to the Sea of Marmara, the marked salinity increase and oligotrophic conditions of the northeastern Mediterranean Sea (~38‰) coincide with the absence of heterothallic reproduction in Mediterranean clones. Notably, these clones failed to mate not only with other populations but also among themselves, showing only rare and sporadic homothallic auxosporulation. It remains unclear whether this reflects environmental adaptation, the sampling of a single mating type, or incipient speciation. Consequently, no conclusions can be drawn regarding reproductive barriers between the Marmara–Black Sea group and the Mediterranean clones.

The shared LSU rDNA ribotype across populations from the Black Sea to the Yellow Sea suggests recent connectivity, but the pan-Eurasian distribution of *N. traheaformis* poses a biogeographical puzzle, consistent with either a wide native range, previously underestimated, or human-mediated introduction. Our current data do not allow us to distinguish between these scenarios, and resolving this question will require population genomic approaches and broader geographic sampling.

Importantly, our conclusions apply specifically to the clonal isolates examined, and we do not exclude the possible presence of genuine *N. navis-varingica* elsewhere in these basins. Continued monitoring using integrative taxonomy is therefore essential for accurate risk assessment. The broader significance of our study lies not merely in documenting new occurrences, but in revising the taxonomic identity of populations previously misidentified as the toxigenic species *N. navis-varingica*, thereby recalibrating the perceived biotoxin risk in the region and underscoring that integrative taxonomy remains indispensable for accurate biodiversity assessment and risk management.

CRediT authorship contribution statement

Nickolai Davidovich: Writing – review & editing, Writing – original draft, Visualization, Methodology, Formal analysis, Conceptualization. **Olga Davidovich:** Visualization, Methodology, Investigation, Data curation. **Svetlana Polyakova:** Visualization, Methodology, Investigation, Data curation. **Elif Eker-Develi:** Writing – original draft, Visualization, Methodology, Data curation. **Vyacheslav Yu. Nikulin:** Writing – original draft, Visualization, Software, Data curation. **Arthur Yu. Nikulin:** Writing – original draft, Visualization, Software, Data curation.

Funding

This work was supported by the Ministry of Science and Higher Education of the Russian Federation within the state assignments (projects 124030100100–0 and 124012400285–7) and by Mersin University (BAP Project 2019–2-AP2–3595).

Declaration of Competing Interest

The authors declare that they have no known competing financial interests or personal relationships that could have appeared to influence the work reported in this paper.

Acknowledgements

The authors thank the reviewers for their helpful comments. We thank Prof. Dr. A.E. Kideys for providing us samples from the Sea of Marmara (Darıca, İzmit Bay). We thank the World Ocean Diatoms Collection at the Karadag Scientific Station for providing facilities and research materials. The grammar and style of the manuscript were refined using DeepSeek AI; this assistance was solely for editorial purposes and did not contribute to text generation or data interpretation. All corrections were manually reviewed and approved by the authors.

Appendix A. Supporting information

Supplementary data associated with this article can be found in the online version at doi:10.1016/j.rsma.2026.105360.

Data availability

Data will be made available on request.

References

Abdullin, Sh.R., Nikulin, A.Y., Bagmet, V.B., Nikulin, V.Y., Gontcharov, A.A., 2021. New cyanobacterium *Aliterella vladivostokensis* sp. nov. (Aliterellaceae, Chroococcidiopsidales), isolated from temperate monsoon climate zone (Vladivostok, Russia). Phytotaxa 527, 221–233. https://doi.org/10.11646/phytotaxa.527.3.7.

Akaike, H., 1974. A new look at the statistical model identification. IEEE Trans. Autom. Control. Comput. Sci. 19, 716–723.

Amato, A., 2010. Species concepts and definitions: reproductive isolation as a tool to reveal species boundaries. Int. J. Plant. Reprod. Biol. 2, 114–126.

Amato, A., Kooistra, W.H.C.F., Montresor, M., 2019. Cryptic diversity: a long-lasting issue for diatomologists. Protist 170, 1–7. https://doi.org/10.1016/j.protis.2018.09.005.

Amato, A., Kooistra, W.H.C.F., Levialdi Ghiron, J.H., Mann, D.G., Pröschold, T., Montresor, M., 2007. Reproductive isolation among sympatric cryptic species in marine diatoms. Protist 158, 193–207. https://doi.org/10.1016/j.protis.2006.10.001.

Andersen, R.A., Berges, J.A., Harrison, P.J., Watanabe, M.M., 2005. Recipes for freshwater and seawater media. In: Andersen, R.A. (Ed.), Algal Culturing Techniques. Elsevier Academic Press, London, pp. 429–538.

Andersen, R.A., Kawachi, M., 2005. Traditional microalgae isolation techniques. In: Andersen, R.A. (Ed.), Algal Culturing Techniques. Elsevier Academic Press, London, pp. 83–100.

Ayaz, F., Eker-Develi, E., Sahin, M., 2018. First report of *Nitzschia navis-varingica* in the Mediterranean Sea and growth stimulatory effects of *Nitzschia navis-varingica*, *Chrysochromulina alifera* and *Heterocapsa pygmaea* on different mammalian cell types. Mol. Biol. Rep. 45, 571–579. https://doi.org/10.1007/s11033-018-4195-7.

Beşiktepe, Ş.T., Sur, H.İ., Özsoy, E., Latif, M.A., Oğuz, T., Ünlüata, Ü., 1994. The circulation and hydrography of the Marmara Sea. Progress. Oceanogr. 34, 285–334. https://doi.org/10.1016/0079-6611(94)90018-3.

Beszteri, B., Ács, É., Medlin, L.K., 2005. Ribosomal DNA sequence variation among sympatric strains of the *Cyclotella meneghiniana* complex (Bacillariophyceae) reveals cryptic diversity. Protist 156, 317–333. https://doi.org/10.1016/j.protis.2005.07.002.

Bonfield, J.K., Smith, K.F., Staden, R., 1995. A new DNA sequence assembly program. Nucleic Acids Res. 23, 4992–4999.

Chepurnov, V.A., Mann, D.G., Sabbe, K., Vyverman, W., 2004. Experimental studies on sexual reproduction in diatoms. Int. Rev. Cytol. 237, 91–154. https://doi.org/10.1016/S0074-7696(04)37003-8.

Darriba, D., Taboada, G.L., Doallo, R., Posada, D., 2012. JModelTest 2: more models, new heuristics and parallel computing. Nat. Methods 9, 772. https://doi.org/10.1038/nmeth.2109.

Daugbjerg, N., Andersen, R.A., 1997. Phylogenetic analyses of the *rbc*L sequences from haptophytes and heterokont algae suggest their chloroplasts are unrelated. Mol. Biol. Evol. 14, 1242–1251. https://doi.org/10.1093/oxfordjournals.molbev.a025733.

Davidovich, N.A., 2001. Species specific sizes and size range of sexual reproduction in diatoms. In: Economou–Amilli, A. (Ed.), Proceedings of the 16th International Diatom Symposium, Athens 2000. University of Athens, Greece, pp. 191–196.

De Luca, D., Piredda, R., Sarno, D., Kooistra, W.H., 2021. Resolving cryptic species complexes in marine protists: phylogenetic haplotype networks meet global DNA metabarcoding datasets. ISME J. 15, 1931–1942.

Dobzhansky, T., 1937. Genetics and the Origin of Species. Columbia University Press, New York.

Eker-Develi, E., Kideys, A.E., 2022. First record of the diatom *Nitzschia navis-varingica* in the Sea of Marmara. Mar. Sci. Technol. Bull. 11, 231–235. https://doi.org/10.33714/masteb.1121995.

Eker-Develi, E., Merve Konucu, M., Tekdal, D., 2020. Analysis of domoic acid within *Nitzschia navis-varingia* and other three *Pseudo-nitzschia* species isolated from the northeastern Mediterranean Sea. International Eurasian Conference on Biotechnology and Biochemistry (BioTechBioChem 2020). Proceeding Book (Abstracts and Full-Text Papers), Ankara, Turkey, pp. 799–806. December 16–18, 2020.

Gallagher, J.C., 1982. Physiological variation and electrophoretic banding patterns of genetically different seasonal populations of *Skeletofunhi cosumnn* (Bacillariophyceae). J. Phycol. 18, 148–162. https://doi.org/10.1111/J.1529-8817.1982.TB03169.X.

Galtier, N., Gouy, M., Gautier, C., 1996. SEAVIEW and PHYLO_WIN: Two graphic tools for sequence alignment and molecular phylogeny. BMC Bioinforma. 12, 543–548. https://doi.org/10.1093/BIOINFORMATICS/12.6.543.

Guillou, L., Chrétiennot-Dinet, M.-J., Medlin, L.K., Claustre, H., Loiseaux-Goër, S., Vaulot, D., 1999. Bolidomonas: a new genus with two species belonging to a new algal class, the Bolidophyceae (Heterokonta). J. Phycol. 35, 368–381.

van Hannen, E.J., Mooij, W., van Agterveld, M.P., Gons, H.J., Laanbroek, H.J., 1999. Detritus-dependent development of the microbial community in an experimental system: qualitative analysis by denaturing gradient gel electrophoresis. Appl. Environ. Microbiol. 65, 2478–2484. https://doi.org/10.1128/AEM.65.6.2478-2484.1999.

Harper, J.T., Saunders, G.W., 2001. The application of sequences of the ribosomal cistron to the systematic and classification of the florideophyte red algae (Florideophyceae, Rhodophyta). Cah. De. Biol. Mar. 42, 25–38. https://doi.org/10.21411/CBM.A.ADC850A3.

Kaczmarska, I., Ehrman, J.M., Moniz, M.B.J., Davidovich, N., 2009. Phenotypic and genetic structure of interbreeding populations of the diatom *Tabularia fasciculata* (Bacillariophyta). Phycologia 48, 391–403. https://doi.org/10.2216/08-74.1.

Kaczmarska, I., Mather, L., Luddington, I.A., Muise, F., Ehrman, J.M., 2014. Cryptic diversity in a cosmopolitan diatom known as *Asterionellopsis glacialis* (Fragilariaceae): implications for ecology, biogeography, and taxonomy. Am. J. Bot. 101, 267–289. https://doi.org/10.3732/ajb.1300306.

Kotaki, Y., Furio, E.F., Bajarias, F.A., Satake, M., Lundholm, N., Koike, K., Sato, S., Fukuyo, Y., Kodama, M., 2006. New stage of the study on domoic acid-producing diatoms–a finding of *Nitzschia navis-varingica* that produces domoic acid derivatives as major toxin components. Coast. Mar. Sci. 30, 116–120.

Kotaki, Y., Koike, K., Yoshida, M., Thuoc, C.V., Huyen, N.T.M., Hoi, N.C., Fukuyo, Y., Kodama, M., 2000. Domoic acid production in *Nitzschia* sp., isolated from a shrimp-culture pond in Do Son, Vietnam. J. Phycol. 36, 1057–1060. https://doi.org/10.1046/j.1529-8817.2000.99209.x.

Kotaki, Y., Lundholm, N., Onodera, H., Kobayashi, K., Bajarias, F.A., Furio, E.F., Iwataki, M., Fukuyo, Y., Kodama, M., 2004. Wide distribution of *Nitzschia navis-varingica*, a new domoic acid-producing benthic diatom found in Vietnam. Fish. Sci. 70, 28–32. https://doi.org/10.1111/j.1444-2906.2003.00766.x.

Kozlov, A.M., Darriba, D., Flouri, T., Morel, B., Stamatakis, A., 2019. RAxML-NG: a fast, scalable and user-friendly tool for maximum likelihood phylogenetic inference. Bioinformatics 35, 4453–4455. https://doi.org/10.1093/bioinformatics/btz305.

Lefebvre, K.A., Robertson, A., 2010. Domoic acid and human exposure risks: A review. Toxicon 56, 218–230. https://doi.org/10.1016/j.toxicon.2009.05.034.

Leigh, J.W., Bryant, D., 2015. POPART: full-feature software for haplotype network construction. Methods Ecol. Evol. 6, 1110–1116. https://doi.org/10.1111/2041-210X.12410.

Lundholm, N., Bates, S.S., Baugh, K.A., Bill, B.D., Connell, L.B., Léger, C., Trainer, V.L., 2012. Cryptic and pseudo-cryptic diversity in diatoms – with descriptions of *Pseudo-nitzschia hasleana* sp. nov. and *P. fryxelliana* sp. nov. J. Phycoljgy 48 436454. https://doi.org/10.1046/j.1529-8817.2000.99210.x.

Lundholm, N., Moestrup, Ø., 2000. Morphology of the marine diatom *Nitzschia navis-varingica*, sp. nov. (Bacillariophyceae), another producer of the neurotoxin domoic acid. J. Phycol. 36, 1162–1174. https://doi.org/10.1111/j.1529-8817.2012.01132.x.

Mann, D.G., Evans, K.M., 2008. The species concept and cryptic diversity. In: Moestrup, Ø. (Ed.), Proceedings of the 12th International Conference on Harmful Algae. International Society for the Study of Harmful Algae and Intergovernmental Oceanographic Commission of UNESCO, Copenhagen, pp. 262–268.

Mann, D.G., Trobajo, R., Sato, S., Li, C., Witkowski, A., Rimet, F., Ashworth, M.P., Hollands, R.M., Theriot, E.C., 2021. Ripe for reassessment: a synthesis of available molecular data for the speciose diatom family Bacillariaceae. Mol. Phylogenetics Evol. 158, 106985. https://doi.org/10.1016/j.ympev.2020.106985.

Mayr, E., 1942. Systematics and the Origin of Species from the Viewpoint of a Zoologist. Columbia University Press, New York.

Moniz, M.B.J., Kaczmarska, I., 2009. Evaluation of nuclear ribosomal RNA and chloroplast gene markers for the DNA taxonomy of centric diatoms. Biochem. Syst. Ecol. 37, 387–399. https://doi.org/10.1016/j.bse.2009.05.004.

Pelusi, A., Romero Martínez, M.L., Mule, A., Scalco, E., Barrenechea Angeles, I., Piredda, R., Kooistra, H.C.F., W., Montresor, M., Sarno, D., 2025. Diatom distribution and long-term survival in a heavily polluted sediment core from the Bay of Bagnoli (Tyrrhenian Sea, Italy). Mediterr. Mar. Sci. 26, 40–54. https://doi.org/10.12681/mms.37946.

Polyakova, S.L., Davidovich, O.I., Podunay, Yu.A., Davidovich, N.A., 2018. Modification of ESAW media used for the cultivation of marine diatoms. Russ. J. Mar. Biol. 3, 73–78. https://doi.org/10.21072/mbj.2018.03.2.06.

Poulíčková, A., Veselá, J., Neustupa, J., Škaloud, P., 2010. Pseudocryptic diversity versus cosmopolitanism in diatoms: a case study on *Navicula cryptocephala* Kütz. (Bacillariophyceae) and morphologically similar taxa. Protist 161, 353–369. https://doi.org/10.1016/j.protis.2009.12.003.

Poulos, S.E., 2020. The Mediterranean and Black Sea Marine System: An overview of its physico-geographic and oceanographic characteristics. Earth-Sci. Rev. 200, 103004. https://doi.org/10.1016/j.earscirev.2019.103004.

Poulos, S.E., 2023. Water masses of the Mediterranean Sea and Black Sea: An Overview. Water 15, 3194. https://doi.org/10.3390/w15183194.

Puilingi, C., Tan, S.N., Maeno, Y., Leaw, C.P., Lim, P.T., Yotsu-Yamashita, M., Terada, R., Kotaki, Y., 2022. First record of the diatom *Nitzschia navis-varingica* (Bacillariophyceae) producing amnesic shellfish poisoning-toxins from Papua New Guinea. Toxicon 216, 65–72. https://doi.org/10.1016/j.toxicon.2022.06.016.

Quijano-Scheggia, S.I., Garcés, E., Lundholm, N., Moestrup, Ø., Andree, K., Camp, J., 2009. Morphology, physiology, molecular phylogeny and sexual compatibility of the cryptic *Pseudo-nitzschia delicatissima* complex (Bacillariophyta), including the description of *P. arenysensis* sp. nov. Phycologia 48, 492–509. https://doi.org/10.2216/08-21.1.

Rambaut, A., Drummond, A.J., Xie, D., Baele, G., Suchard, M.A., 2018. Posterior summarization in bayesian phylogenetics using tracer 1.7. Syst. Biol. 67, 901–904. https://doi.org/10.1093/sysbio/syy032.

Romero, M.L.J., Lirdwitayaprasit, T., Kotaki, Y., Lundholm, N., Relox, J., Jr, Furio, E.F., Terada, R., Yokoyama, T., Kodama, M., Fukuyo, Y., 2008. Isolation of ASP toxin-producing *Nitzschia navis-varingica* from Thailand. Mar. Res. Indones. 33, 225–228. https://doi.org/10.14203/mri.v33i2.498.

Ronquist, F., Huelsenbeck, J.P., 2003. MrBayes 3: Bayesian phylogenetic inference under mixed models. Bioinformatics 19, 1572–1574. https://doi.org/10.1093/bioinformatics/btg180.

Saçu, Ş., Şen, O., Erdik, T., 2025a. Hydrodynamics of the Turkish Strait System: Insights from 35 years of three-dimensional numerical model simulation. Reg. Stud. Mar. Sci. 89, 104315. https://doi.org/10.1016/j.rsma.2025.104315.

Saçu, Ş., Şen, O., Erdik, T., 2025b. Hydrodynamics of the Turkish Strait System: Insights from 35 years of three-dimensional numerical model simulation. Reg. Stud. Mar. Sci. 89, 104315. https://doi.org/10.1016/j.rsma.2025.104315.

Scholin, C.A., Herzog, M., Sogin, M., Anderson, D.M., 1994. Identification of group- and strain-specific genetic markers for globally distributed Alexandrium (Dinophyceae). II. Sequence analysis of a fragment of the LSU rRNA gene. J. Phycol. 30, 999–1011.

Smida, D.B., Lundholm, N., Kooistra, W.H., Sahraoui, I., Ruggiero, M., Kotaki, Y., Ellegaard, M., Lambert, C., Mabrouk, H.H., Hlaili, A.S., 2014. Morphology and molecular phylogeny of *Nitzschia bizertensis* sp. nov. – A new domoic acid-producer. Harmful Algae 32, 49–63. https://doi.org/10.1016/j.hal.2013.12.004.

Stamatakis, A., Hoover, P., Rougemont, J., 2008. A rapid bootstrap algorithm for the RAxML web servers. Syst. Biol. 57, 758–771. https://doi.org/10.1080/10635150802429642.

Suriyanti, S.N.P., Usup, G., 2015. First report of the toxigenic *Nitzschia navis-varingica* (Bacillariophyceae) isolated from Tebrau Straits, Johor, Malaysia. Toxicon 108, 257–263. https://doi.org/10.1016/j.toxicon.2015.10.017.

Tamura, K., Stecher, G., Kumar, S., 2021. MEGA11: molecular evolutionary genetics analysis Version 11. Mol. Biol. Evol. 38, 3022–3027.

Tan, S.N., Kotaki, Y., Teng, S.T., Lim, H.C., Gao, C., Lundholm, N., Wolf, M., Gu, H., Lim, P.T., Leaw, C.P., 2025. Intraspecific genetic diversity with unrestricted gene flow in the domoic acid-producing diatom *Nitzschia navis-varingica* (Bacillariophyceae) from the Western Pacific. Harmful Algae 141, 102769. https://doi.org/10.1016/j.hal.2024.102769.

Tan, S.N., Teng, S.T., Lim, H.C., Kotaki, Y., Bates, S.S., Leaw, C.P., Lim, P.T., 2016. Diatom *Nitzschia navis-varingica* (Bacillariophyceae) and its domoic acid production from the mangrove environments of Malaysia. Harmful Algae 60, 139–149. https://doi.org/10.1016/j.hal.2016.11.003.

Wang, Y., Wang, J., Chen, Y., Liu, S., Zhao, Y., Chen, N., 2022. Comparative analysis of bacillariophyceae chloroplast genomes uncovers extensive genome rearrangements associated with speciation. Int. J. Environ. Res. Public. Health 19, 10024. https://doi.org/10.3390/ijerph191610024.

Witkowski, A., Li, C.L., Zgłobicka, I., Yu, S.X., Ashworth, M., Dąbek, P., Qin, S., Tang, C., Krzywda, M., Ruppel, M., Theriot, E.C., Jansen, R.K., Car, A., Płociński, T., Wang, Y. C., Sabir, J.S.M., Daniszewska-Kowalczyk, G., Kierzek, A., Hajrah, N.H., 2016. Multigene assessment of biodiversity of diatom (Bacillariophyceae) assemblages from the littoral zone of the Bohai and Yellow Seas in Yantai region of northeast China with some remarks on ubiquitous taxa. J. Coast. Res. 74, 166–195. https://doi.org/10.2112/SI74-016.1.